Korean J. Chem. Eng., 32(6), 1137-1141 (2015)
DOI: 10.1007/s11814-014-0285-y

pISSN: 0256-1115
eISSN: 1975-7220

Synthesis, characterization and bactericidal property of chitosan-graft-polyaniline/montmorillonite/ZnO nanocomposite

Alireza Samzadeh-Kermani† and Somayeh Miri

Department of Chemistry, Faculty of Science, University of Zabol, Zabol, Iran
(*Received 31 May 2014 / accepted 23 September 2014*)

Abstract−We synthesized the nanocomposite of chitosan-graft-polyaniline/montmorillonite/zinc oxide (CTS-g-PANi/MMT/ZnO). ZnO nanoparticles (NPs) were successfully synthesized from ZnO powder in the Cts/MMT matrix, using traditional method. CTS-g-PANi co-polymer was synthesized in the presence of ammonium peroxydisulfate (APS). The CTS-g-PANi and MMT were used as the natural polymeric stabilizer and the solid support, respectively. The morphology and the particle size of ZnO NPs and synthesized nanocomposite were investigated by Fourier-transform infrared (FT-IR) spectroscopy, X-ray diffraction (XRD) analysis, and scanning electron microscopy (SEM). According to the XRD results, the nanoparticle size was found to be in the range of 22-35 nm. SEM images showed the hexagonal shape of ZnO NPs, which is suitable for the evaluation of antibacterial activity. Finally, the bactericidal property of prepared nanocomposites was also evaluated against the bacteria of Gram positive *Staphylococcus aureus* (*Staph.*) and Gram negative *Escherichia coli* (*E. coli*), using the paper disc diffusion method.

Keywords: ZnO Nanoparticles, Nanocomposites, Montmorillonite, Chitosan-grafted-polyaniline, Bactericidal

INTRODUCTION

Nanotechnology is fundamentally about the preparation of nanoscale materials [1]. Nanoparticles exhibit new and improved characteristics based on morphology, size and distribution respecting larger particles from which they are made [2]. Among different nanomaterials, ZnO nanoparticles possess a special status due to their high specific surface area, optical transparency, bio-compatibility, non-toxicity, chemical and photochemical stability, convenient fabrication, high-electron communication features and electrochemical activities [3]. ZnO NPs are extensively used in producing bioceramics [4], porous ceramic parts employed in drug delivery systems [5], nanocomposite biosensors [6], nanocomposite membranes [7], catalysts for liquid phase hydrogenation [8], UV shielding materials [9] and chemical adsorbents [10]. Recently, ZnO NPs have been synthesized via a wide variety of physical and chemical methods, such as homogeneous precipitation [11], hydrothermal synthesis [12], sol-gel process [13] or electrodeposition [14]. Our main objective was to synthesize a new nanocomposite based on ZnO NPs, CTS-g-PANi and MMT. ZnO NPs were prepared using chemical reduction method which is fast, simple and low cost. Finally, the bactericidal property of the synthesized nanocomposites was evaluated against two pathogenic bacteria of gram positive *Staphylococcus aureus* (*Staph.*) and gram negative *Escherichia coli* (*E. coli*). Polyaniline (PANi) has been extensively studied because of its facile synthesis, environmental stability, electrical, electrochemical and optical properties, and has found applications in antistatic and anticorrosion coatings, biological and chemical sensors, electrodes for light-emitting diodes and batteries [15]. Chitosan (CTS), a polysaccharide biopolymer, which is linked through β-D-1-4-glycosidic bonds units [16], IS derived from naturally occurring chitin, and an excellent natural polymer due to its nontoxicity, biodegradability, biocompatibility, bioactivity, multifunctional groups and antimicrobial activity. Furthermore, CTS is extensively being investigated in field of agriculture, food packaging industry, bone engineering, artificial skin, biomedical material and drug delivery [17]. Grafting of CTS allows the formation of functional derivatives by covalent binding of a molecule (the graft) on the CTS backbone. Studies have also shown that after primary derivation followed by graft modification, CTS would obtain much improved water solubility and bioactivities such as antibacterial and antioxidant properties [18]. Recent advances in clay polymer nanocomposites have shown that exfoliated dispersions of montmorillonite clay in polymer matrix can lead to significantly enhanced toughness and barrier resistance [19]. Clay has been used as a carrier of antibacterial inorganic material with favorable results, because it has a high ion-exchange capacity, high surface area, high absorptive capacity, a negative surface charge, chemical inertness and low or null toxicity [20]. Polymer layered silicate (PLS) nanocomposites have the potential of being a low-cost high-performance composites. Amongst layered silicate nanoparticles, montmorillonite (MMT) has high-aspect ratio and high-surface area that could lead to great property enhancements [21].

MATERIALS AND CHEMICALS

1. Materials

All materials were of laboratory grade chemicals. Zinc Oxide powder as the source of ZnO NPs, MMT as the solid support and Chitosan as the natural polymeric stabilizer, were supplied by Merck.

†To whom correspondence should be addressed.
E-mail: arsamzadeh@yahoo.com, arsamzadeh@uoz.ac.ir

PANi was synthesized from aniline, in the presence of APS in acetic acid. The bactericidal property of synthesized NPs and nanocomposites was carried out using two different bacterial strains including Gram positive *Staphylococcus aureus* and Gram negative *Escherichia coli*, which were obtained from Faculty of Pharmacy, Zabol University of Medical Sciences, Zabol, Iran.

2. Chemicals

2-1. Preparation of ZnO Nanoparticles

First, 0.1-1 g ZnO powder was dissolved in 100 ml of 1% acetic acid and the solution was sonicated for 30 min to obtain Zn^{2+} cations. Then, 50 ml of 1 M $NaOH_{(aq)}$ was added dropwise and stirred until the solution attained pH=10. The solution was heated in a water bath at 40-80 °C for 3 h. At this time the solution was filtered and washed three times by distilled water, and then dried in an oven at 50 °C for 1 h according to the conventional procedure [22].

2-2. Synthesis of Cts-g-PANi

Chemical graft reaction was carried out in a 100 ml three-necked round bottom flask equipped with thermometer, condenser and gas inlet. First 0.4 g of CTS was added to 30 ml acetic acid 2% with constant stirring under Argon atmosphere for 1 h. A solution of 1.23 g ammonium persulfate in 20 ml distilled water was added to the flask at 0-5 °C. Then 0.5 g of aniline was added dropwise and suspended into 10 ml of distilled water. The reaction was completed at room temperature with magnetic stirring. After a further 12 h continuous stirring, the mixture became a black solution containing CTS-g-PANi copolymer.

2-3. Synthesis of Cts /MMT/ZnO

First, a solution of CTS (100 ml, 0.5 wt%) was prepared by dissolving in 1.0 wt% of acetic acid solution (pH~3.53) under constant stirring for 45 min for each sample. ZnO NPs were added to each CTS sample under constant stirring to prepare a suspension. While ZnO NPs′ concentration was increased, the suspension color was changed to a darkened solution. The concentrations of ZnO NPs in these samples were 0.5% (C1), 1.0% (C2), 1.5% (C3) and 2.0% (C4). Constant amounts of MMT were added to different samples and stirred for 24 h at room temperature to obtain the CTS/MMT/ZnO suspensions.

2-4. Synthesis of CTS-g-PANi/MMT/ZnO Nanocomposites

The suspension of CTS /MMT/ZnO was added to the solution of CTS-g-PANi, and the solution of CTS-g-PANi/MMT/ZnO was obtained and then centrifuged, washed three times by double-distilled water to remove the silver ion residues, then was dried at 40 °C under vacuum for 24 h. All experiments were implemented at an ambient temperature.

CHARACTERIZATION

1. Instrumental Analysis

All products were analyzed by Fourier transform infrared (FT-IR) spectroscopy (Bruker Optics Ft Tensor 27, Germany) using KBr discs. The X-ray diffraction (XRD) analysis was also conducted by using a Bruker D8 X-ray diffractometer. SEM was applied to observe the surface morphology of CTS-g-PANi/MMT/ZnO nanocomposites using a Hitachi S4160 instrument. Thin films of the samples were prepared on graphite adhesives; then, the surface of samples was coated by gold powder using sputter hammer instrument. The ^{1}H-NMR spectrum of Cts-g-PANi was recorded at 400 MHz on a Bruker spectrometer. NMR data are reported in the order of chemical shift (ppm), spin multiplicity, and integration.

2. Bactericidal Property

The bactericidal property of ZnO NPs was investigated against *Staphylococcus aureus (Staph.)* and *Escherichia coli (E. coli)* microorganisms by disk diffusion method in accordance with the proce-

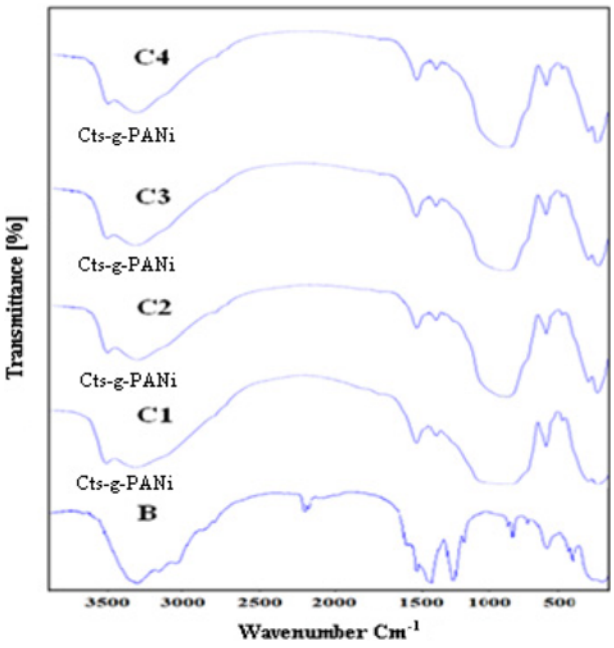

Fig. 1. FT-IR spectra of prepared ZnO NPs (B), nanocomposites 0.5% (C1), 1.0% (C2), 1.5% (C3) and 2.0% (C4).

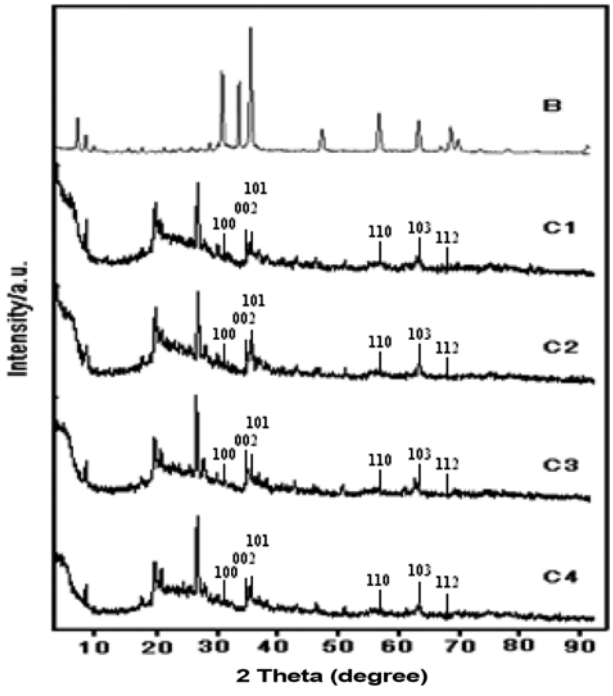

Fig. 2. XRD spectra of prepared ZnO NPs (B) and nanocomposites 0.5% (C1), 1.0% (C2), 1.5% (C3) and 2.0% (C4).

dure described by Hwang and Ma [23]. This method is a means of measuring the effect of an antimicrobial agent against bacteria growth in a culture. The Muller-Hinton agar (MHA) powder was applied as a culture medium for bacteria growth. To prepare the culture medium, 19 g of agar was dissolved into 500 ml of distilled water and the transparent brown solvent was achieved via boiling the solution. The MHA medium (15 ml) was sterilized at 120 °C for 60 min in autoclave, cooled to room temperature, and then poured into sterilized petri dishes (10-90 mm). After cooling over 24 h, the bacteria of interest were swabbed uniformly across the culture plate. Filter-paper disks were placed on the surface of agar. To investigate bactericidal property, 40 µl of each concentration of the samples was dropped on disks' surface by a sampler. If the compounds are effective against the bacteria at a certain concentration, then no colonies will grow and the concentration in the agar is greater than or equal to the effective concentration. This region is called the zone of inhibition. The size of the inhibition zone measures the effectiveness of the compounds. A more effective compound produces a larger clear area around the disk. All of the tests were done under laminar flow hood. Finally, all petri dishes containing bacteria and antibacterial reagents were incubated at 37 °C for 24 h. At the end of the incubation period, the diameters of the inhibition zones formed around each disk were determined and presented in mm. The results concerning antibacterial activity were expressed as strong activity (>13 mm), moderate activity (6-12 mm), weak activity (5 mm) or no activity (inhibition zone <5 mm).

RESULT AND DISCUSSION

1. FT-IR Spectroscopy

FT-IR spectra of ZnO NPs and nanocomposites are shown in Fig. 1. The IR spectrum of chitosan has a strong peak around 3,480 cm^{-1} due to the stretching vibration of O-H, inter hydrogen bonding, and the extensive vibration of N-H. In the CTS-g-PANi copo-

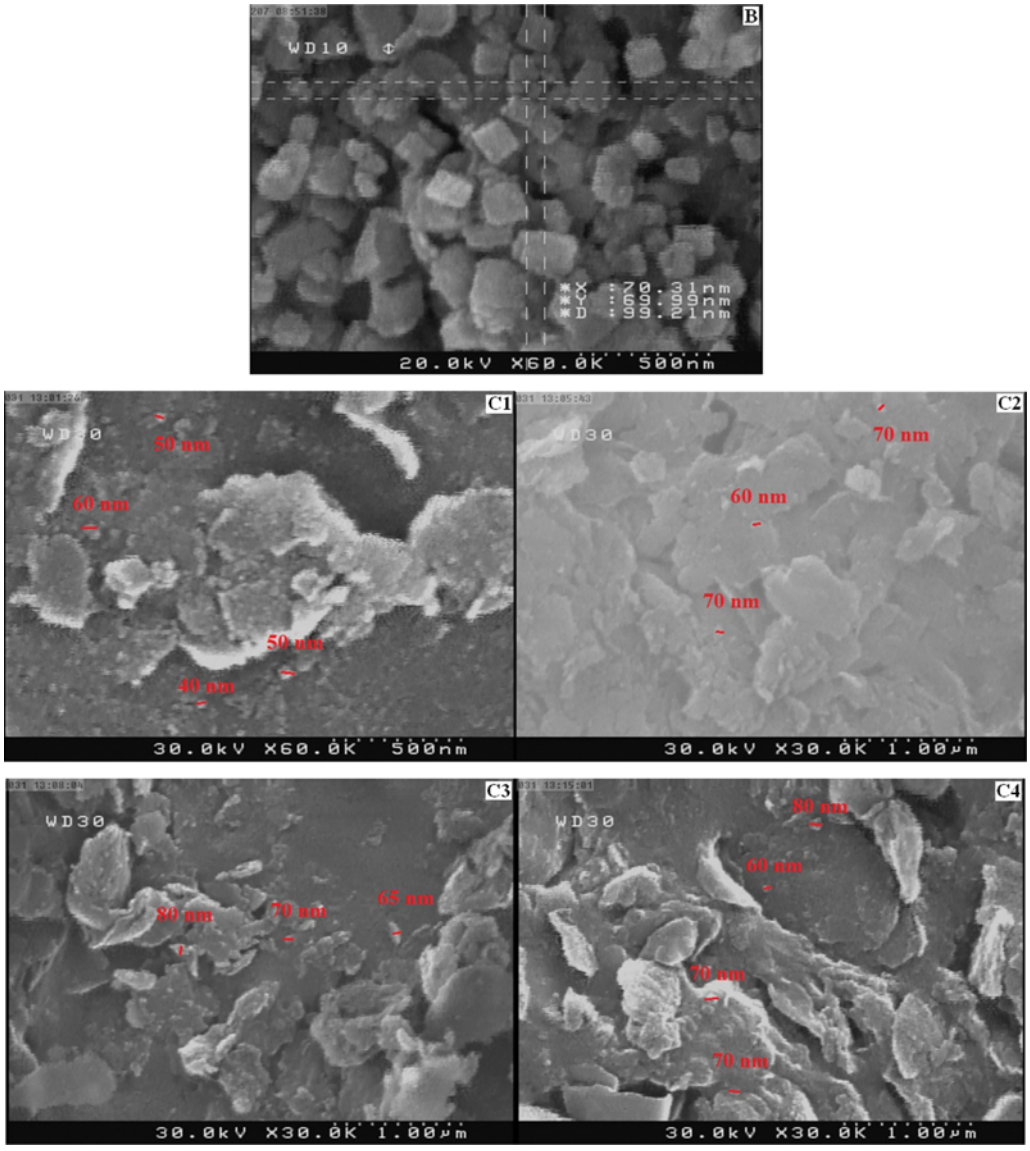

Fig. 3. SEM images of ZnO NPs (B) and nanocomposites 0.5% (C1), 1.0% (C2), 1.5% (C3) and 2.0% (C4).

lymer, the peak at 3,200-3,500 cm^{-1} is of quite reduced intensity and broad (due to overlapping of O-H groups in CTS with N-H groups in PANi), which is shown in the IR spectra of C1 to C4. Reduced intensity of this peak with respect to CTS shows that appreciable amounts of O-H and N-H groups at CTS have been grafted with PANi chain. The peak at 3,100 cm^{-1} (Ar-H stretching of PANi) is overlapped with the O-H stretching of chitosan [24]. The free OH functional group has a broad peak at 3,600-3,650 cm^{-1}, and this peak moves to 3,200-3,500 cm^{-1}, if the OH group is engaged in the formation of hydrogen bond or complex with metal particles. An intense peak at 1,000-1,350 cm^{-1} shows the C-N bond existence in polyaniline chains. The presence of benzene rings in polyaniline structure is also confirmed with an intense tensile peak around 1,500 cm^{-1}. The IR spectrum of the nanocomposite shows other peaks assigned to the chitosan around 1,148, 1,012, and 879 cm^{-1} and PANi around 1,593, 1,504 and 1,303 cm^{-1}. From IR data, it is clear that the CTS-g-PANi copolymer has characteristic peaks of PANi and of chitosan, which can be a strong evidence for grafting.

2. XRD Analysis

The X-ray beam was Ni-filtered Cu Kα radiation from a sealed tube. CTS-g-PANi/MMT/ZnO nanocomposites were analyzed in a 2θ range of 1-70°, and the scanning rate was 1.5°/min. Pure CTS showed two peaks at 2θ of 9.37°, 19.56° and a broad peak appearing at 2θ values in the range of 19-28° was generally pertinent to the polymeric PANi chains. The peaks at 2θ values of 7.12° for MMT and 6.09° for MMT/CTS were also observed. The sharp and intense peaks around 2θ values of 31.7, 34.36, 36.2, 56.59, 62.8, 67.90 and with 100, 002, 101, 110, 103, 112 diffraction respectively, were related to ZnO crystalline hexagonal structure which formed a benign stabilizing complex with polymeric matrix. All of the diffraction peaks were in good agreement with those of hexagonal wurtzite structure of ZnO (JCPDS card 36-1451) [25]. The XRD patterns were clearly exhibited the presence of ZnO NPs in nanocomposites C1, C2, C3 and C4 (Fig. 2). The average particle size of the CTS-g-PANi/MMT/ZnO nanocomposites was calculated using Scherrer's Equation:

$$D = \frac{K\lambda}{\beta \cos\theta}$$

where D is the crystallite size, k is the shape factor that assumes a value of 0.89 for ZnO, λ is the wavelength of the Cu Kα radiation (0.154 nm), β is the full-width at half-maximum of the diffraction peaks and θ is the diffraction angle [26].

3. FESEM Analysis

SEM images show that the samples with medium concentrations have a better size distribution (Fig. 3). This is because the particles are less aggregated in medium concentrations of the samples, and therefore the particles' sizes are smaller than those of higher concentrations of ZnO NPs. Also, this fact confirms the results of XRD analyses.

4. ^{1}H-NMR Spectroscopy

Fig. 4 shows the ^{1}H-NMR spectrum of Cts-g-PANi, in which the signal at 1.91 ppm indicates different protons of CH_2 in the main chain CTS. The signal at 2.5 ppm is probably related to the C-H protons on CTS which are overlapped with the peak of DMSO protons. The signal at 3.4 ppm is the hydroxyl group peak along the chain that is overlapped with the H_2O protons. Therefore, the other broad signal at the range 6.97-7.48 ppm pertains to the aromatic protons of PANi.

5. Antibacterial Activity of Prepared CTS-g-PANi/MMT/ZnO Nanocomposites

The results of the bactericidal property of NPs and nanocom-

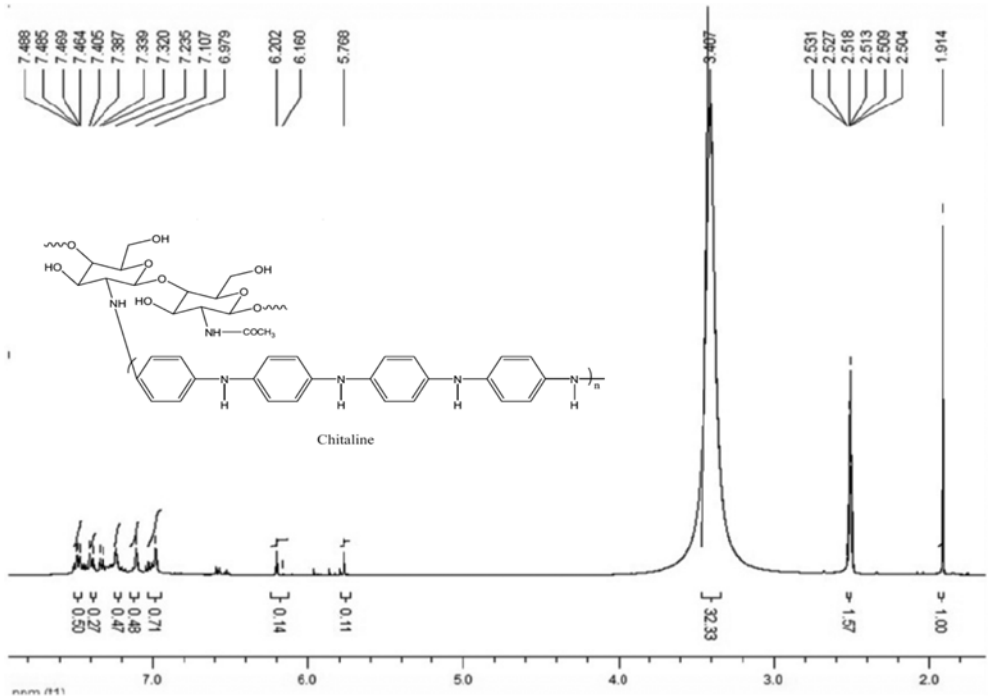

Fig. 4. ^{1}H-NMR spectrum of CTS-g-PANi.

Table 1. Average inhibition zone and standard deviation for ZnO NPs and various concentrations of nanocomposites 0.5% (C1), 1.0% (C2), 1.5% (C3) and 2.0% (C4)

Sample	Formation diagonal circulars	
	Escherichia coli (*E. coli*)	*Staphylococcus aureus* (*Staph.*)
ZnO	20 mm	21 mm
0.5%	13 mm	15 mm
1.0%	15 mm	17 mm
1.5%	17 mm	19 mm
2.0%	11 mm	13 mm

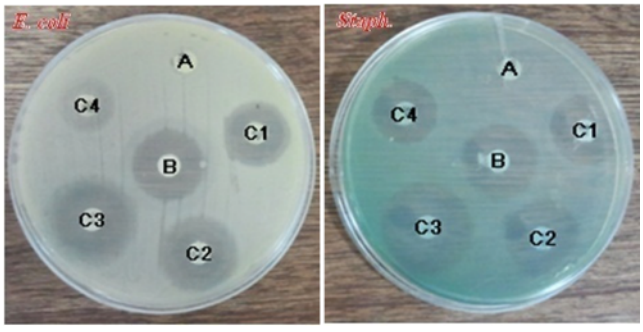

Fig. 5. A schematic illustration of created inhibition zones for antibacterial activity of CTS-g-PANi (A), ZnO NPs (B) and various concentrations of nanocomposites 0.5% (C1), 1.0% (C2), 1.5% (C3) and 2.0% (C4).

posites against on two bacteria are depicted in Table 1. The inhibition zone increased with increasing ZnO NPs′ content of nanocomposites, and also the inhibition zone for *Staph.* was greater than that for *E. coli* (Fig. 5). However, the bactericidal property could be attributed to thte bactericidal effect of ZnO NPs. The bactericidal property of nanocomposites containing low and high concentrations of ZnO NPs, was low. It was due to the presence of small amounts of ZnO NPs in low concentration nanocomposite (C1), and agglomeration of NPs in high concentration nanocomposite (C4). At this circumstance the amount of interaction with cell membrane was decreased and caused a reduction in the inhibition zone.

CONCLUSION

ZnO NPs were synthesized from ZnO powder. CTS-g-PANi/MMT/ZnO nanocomposites were prepared in different concentrations of NPs [0.5% (C1), 1.0% (C2), 1.5% (C3) and 2.0% (C4)]. Nanocomposites containing different sizes of NPs showed strong bactericidal activity against Gram-positive and Gram-negative bacteria. These results showed that the antibacterial resistance of ZnO NPs in nanocomposites could be modified according to their size distribution, and decreased with increasing in particle size due to agglomeration (C4). Moreover, the XRD analysis peaks for ZnO NPs were in good agreement with those of hexagonal wurtzite structure. SEM images showed a proper size distribution of NPs in nanocomposites C2 and C3. The size distribution for of nanocomposites of different concentrations was in the range 22.3-34.8 nm. Further studies should be focused on the investigation of cytotoxic effects and also the bactericidal effects of CTS-g-PANi/MMT/ZnO nanocomposites against different types of bacteria for potential broadening of their applications, such as in drug-delivery.

ACKNOWLEDGEMENT

This study has been accomplished under financial support of the Department of Chemistry, University of Zabol and cordially laboratorial collaboration of the Faculty of Pharmacy, Zabol University of Medical Sciences, which should be appreciated.

REFERENCES

1. B. Zhou, R. Balee and R. Groenendaal, *Nanotechnol. L. Bus.*, **2**, 222 (2005).
2. C. J. Murphy, *J. Mater. Chem.*, **18**, 2173 (2008).
3. S. Singh, S. Arya, P. Pandey, B. Malhotra, S. Saha, K. Sreenivas and V. Gupta, *Appl. Phys. Lett.*, **91**, 63901 (2007).
4. R. M. B. Faria, D. B. César and V. M. M. Salim, *Catal. Today*, **168**, 133 (2008).
5. Y. W. Sun and Y. Y. Tsui, *Opt. Mater.*, **29**, 1111 (2007).
6. X. Ren, D. Chen, X. Meng, F. Tang, X. Hou, D. Han and L. Zhang, *J. Colloid Interface Sci.*, **183**, 334 (2009).
7. J. Wang, P. Liu, S. Wang, W. Han, X. Wang and X. Fu, *J. Mol. Catal. A: Chem.*, **21**, 273 (2007).
8. A. Renken and L. Kiwi-Minsker, *Adv. Catal.*, **47**, 53 (2010).
9. A. Anžlovar, Z. Crnjak Orel and M. Žigon, *Eur. Polym. J.*, **46**, 1216 (2010).
10. H. F. Garces, H. M. Galindo, L. J. Garces, J. Hunt, A. Morey and S. L. Suib, *Micropor. Mesopor. Mater.*, **127**, 190 (2010).
11. K. D. Kim, D. N. Han, J. B. Lee and H. T. Kim, *Scripta Mater.*, **54**, 143 (2006).
12. W. J. Li, E. W. Shi, Y. Q. Zheng and Z. W. Yin, *J. Mater. Sci. Lett.*, **20**, 1381 (2001).
13. K. D. Kim and H. T. Kim, *J. Sol-Gel Sci. Technol.*, **25**, 183 (2002).
14. B. O'Regan, D. T. Schwartz, S. M. Zakeeruddin and M. Gratzel, *Adv. Mater.*, **12**, 1263 (2000).
15. (a) A. G. MacDiarmid, *Angew. Chem. Int. Ed.*, **40**, 2581 (2001); (b) R. L. Elsenbaumer, J. R. Reynolds and T. A. Skotheim, *Handbook of Conducting Polymers, Marcel Dekker* (1998).
16. S.-K. Kim and E. Mendis, *Food Res. Int.*, **39**, 383 (2006).
17. R. K. MNV, *React. Funct. Polym.*, **46**, 1 (2000).
18. M. Ignatova, N. Manolova and I. Rashkov, *Eur. Polym. J.*, **43**, 1112 (2007).
19. Y. Zhong and S. Q.Wang, *J. Rheol.*, **47**, 483 (2002).
20. D. Zhao, J. Zhou and N. Liu, *Appl. Clay Sci.*, **33**, 161 (2006).
21. Q. T Nguyen and D. G. Baird, *Adv. Polym. Technol.*, **25**, 270 (2006).
22. M. AbdElhady, *Int. J. Carbohyd. Chem.*, **6**, 2012 (2012).
23. J. J. Hwang and T. W. Ma, *Mat. Chem. Phys.*, **136**, 613 (2012).
24. S. H. Hosseini, J. Simiari and B. Farhadpour, *Iran. Polym. J.*, **18,** 3 (2009).
25. M. Guo, P. Diao and S. Cai, *J. Solid State Chem.*, **178**, 1864 (2005).
26. J. F. Zhu and Y. J. Zhu, *J. Phys. Chem. B.*, **110**, 8593 (2006).